New Platinum Complexes from Salen- and Hydroxy-Substituted Salpn-Naphthalene Ligands with CO_2 Reduction Activity

Javier O. Rivera-Reyes [1,2], Joesene Soto-Pérez [1,2], Miguel Sepulveda-Pagán [3], Linguo Lu [1], Justin Borrero-Negrón [3], Alanys V. Luna-Ramírez [1,2], Pedro Trinidad-Pérez [1,2], Yomaira Pagán-Torres [3], Zhongfang Chen [1], Carlos R. Cabrera [4], William C. West [5], John-Paul Jones [5] and Dalice M. Piñero Cruz [1,2,*]

[1] Chemistry Department, College of Natural Sciences, Rio Piedras Campus, University of Puerto Rico, P.O. Box 23346, San Juan, PR 00931-3346, USA; javier.rivera19@upr.edu (J.O.R.-R.);
[2] Molecular Science Research Center, University of Puerto Rico, 1390 Ponce de León, San Juan, PR 00926, USA
[3] Department of Chemical Engineering, University of Puerto Rico-Mayagüez Campus, Mayagüez, PR 00681-9000, USA
[4] Department of Chemistry, University of Texas, El Paso, 500 West University Avenue, El Paso, TX 79968, USA
[5] Jet Propulsion Laboratory, California Institute of Technology, Pasadena, CA 91109, USA
* Correspondence: dalice.pinero@upr.edu

Table of Contents

NMR

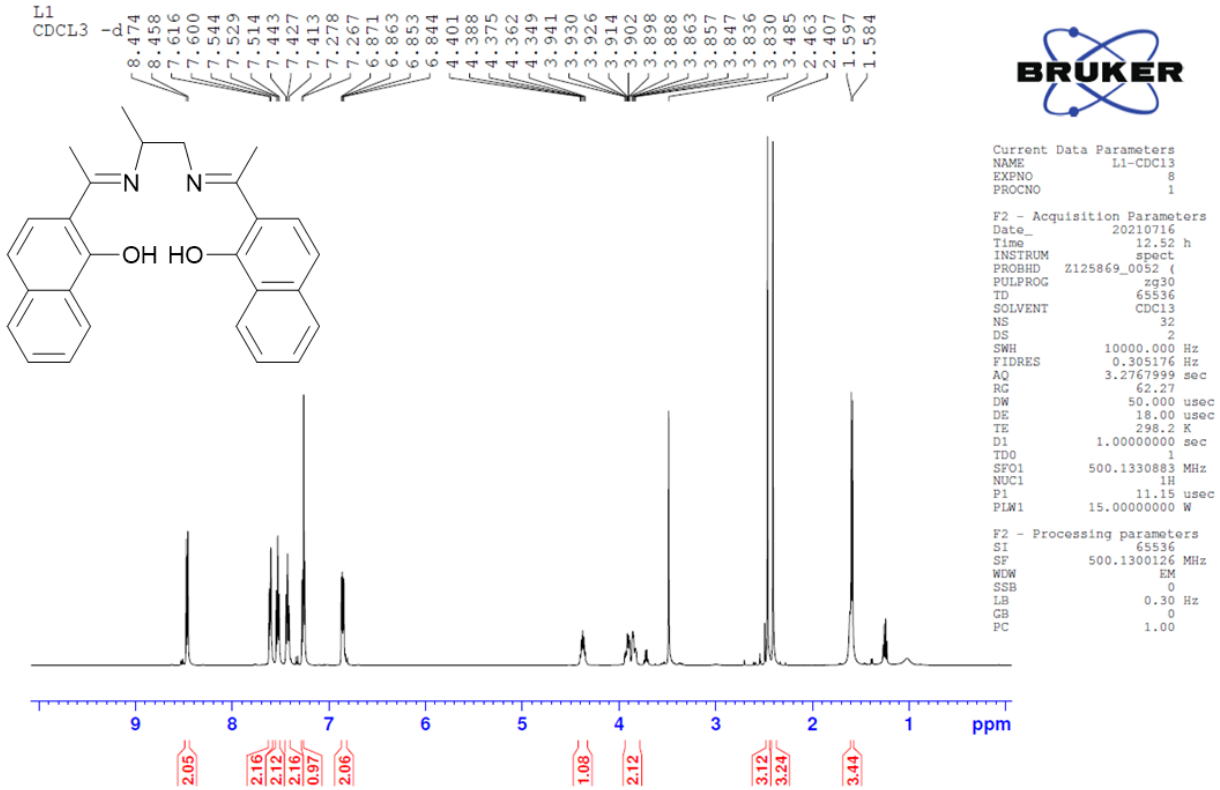

Figure S1: ^{1}H-NMR in $CDCl_3$ of **L1.**

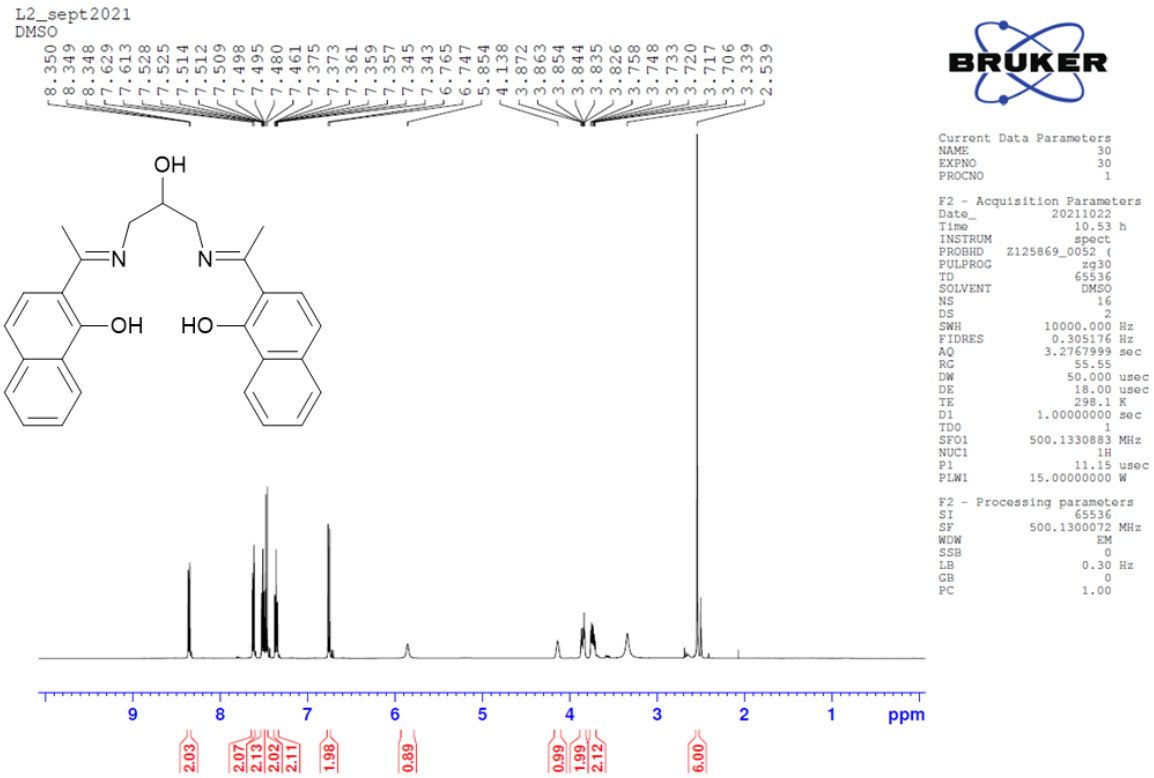

Figure S2: ^{1}H-NMR in DMSO of **L2**.

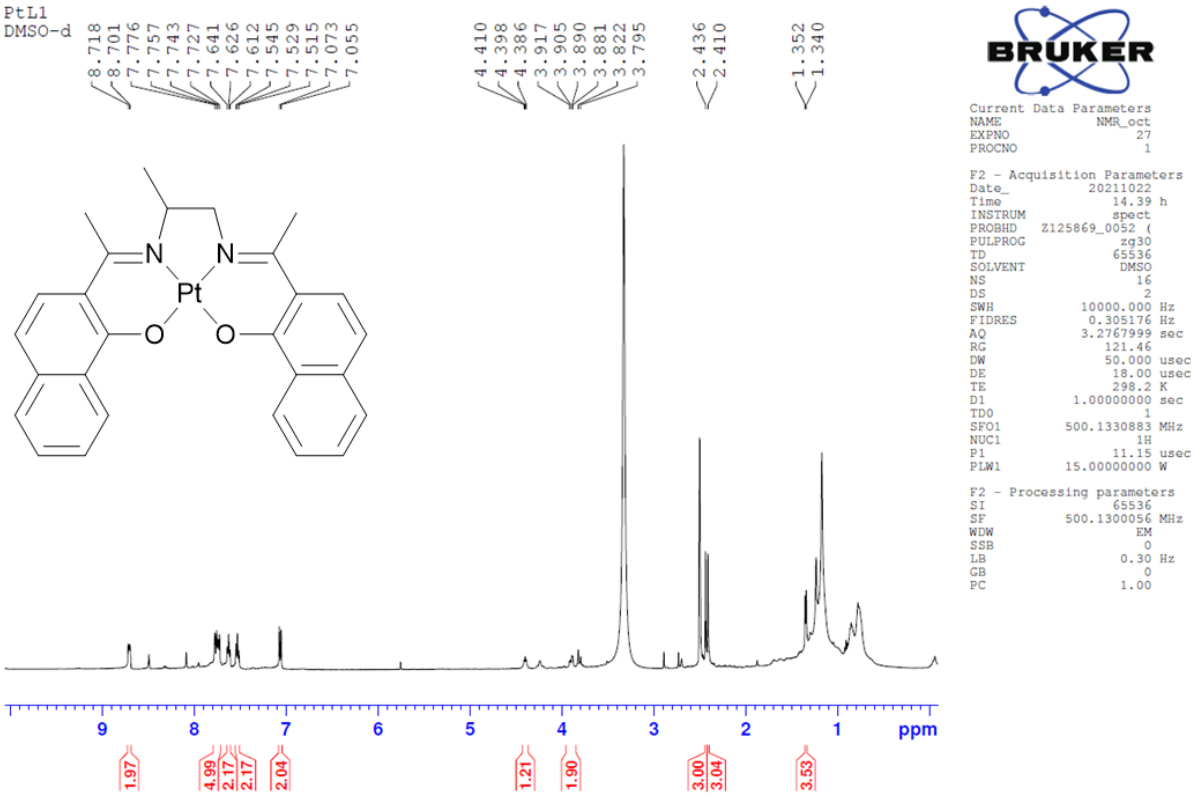

Figure S3: ^{1}H-NMR in DMSO of **PtL1**.

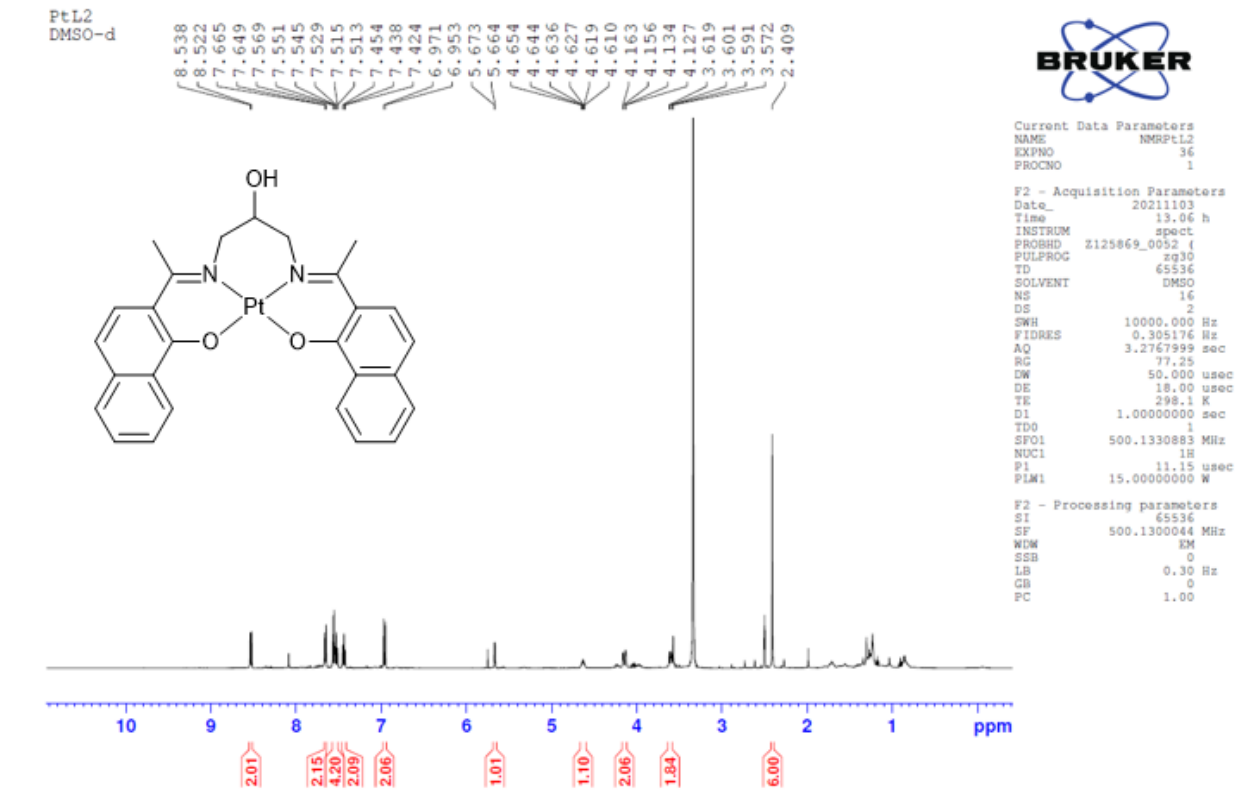

Figure S4: ^{1}H-NMR in DMSO of **PtL2**.

FTIR

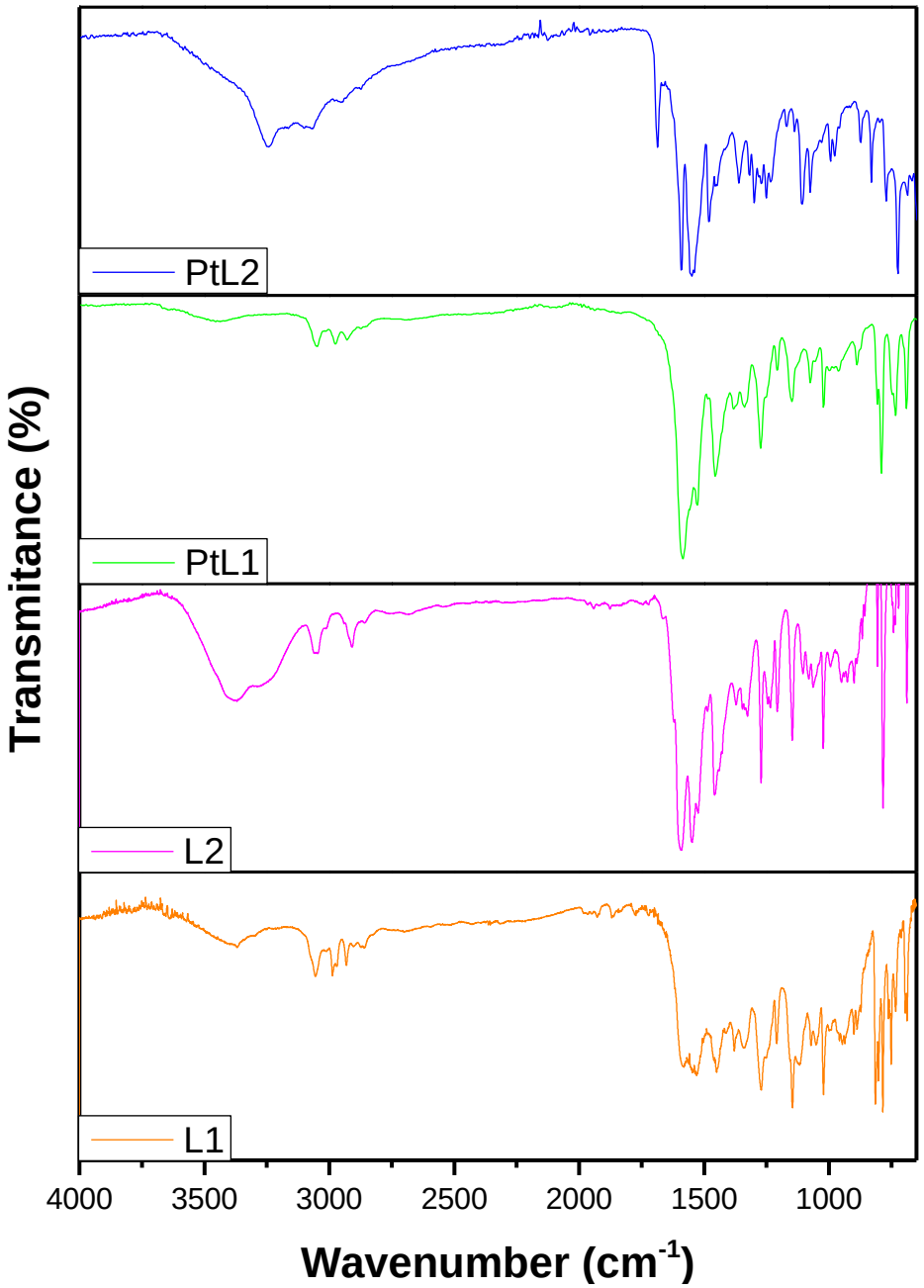

Figure S5: FTIR spectra of **PtL2, PtL1, L2,** and **L1.**

UV-Vis

Compound	λ_{max} (nm)	ε (dm³ mol⁻¹ cm⁻¹)
L1	325	2990
	416	5639
	434	5259
L2	332	7995
	385	3134
	408	4383
	432	4901
PtL1	323	8898
	434	2209
	460	1751
PtL2	302	12270
	427	3908
	442	3720

Table S1: Lambda max (λ_{max}) and molar absorptivity coefficient (ε) of all compounds.

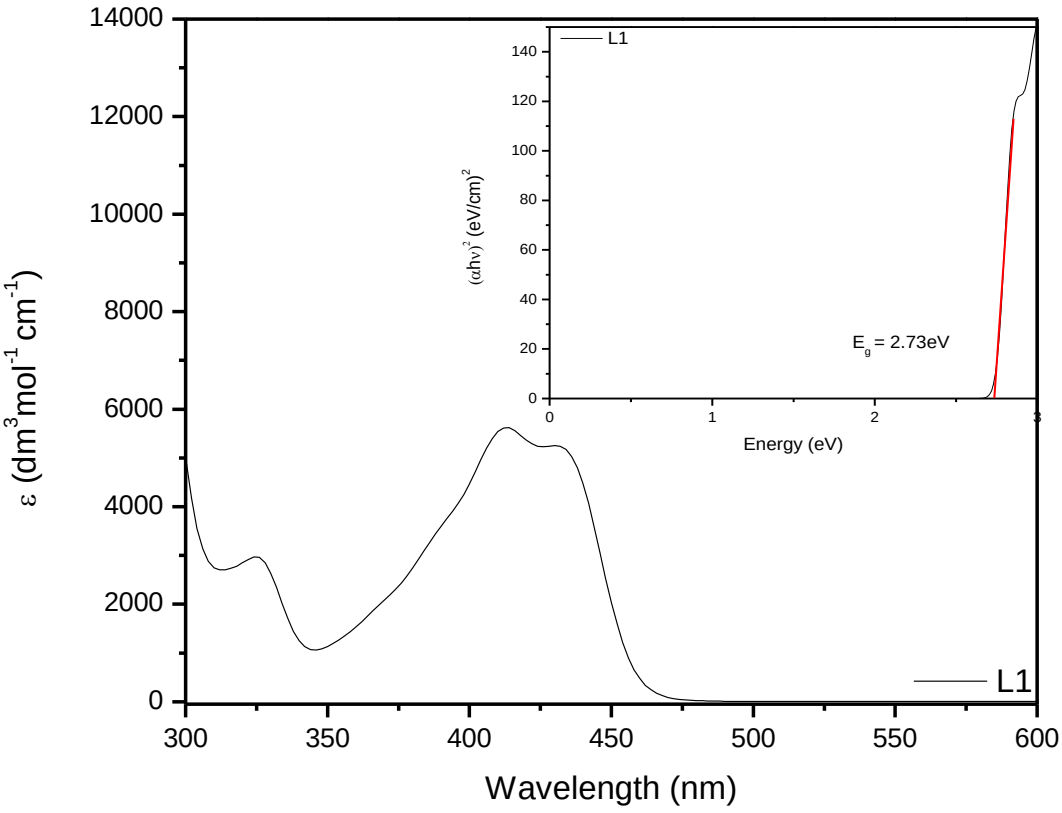

Figure S6: UV-Vis spectra and Tauc plot of **L1** [21, 29, 32].

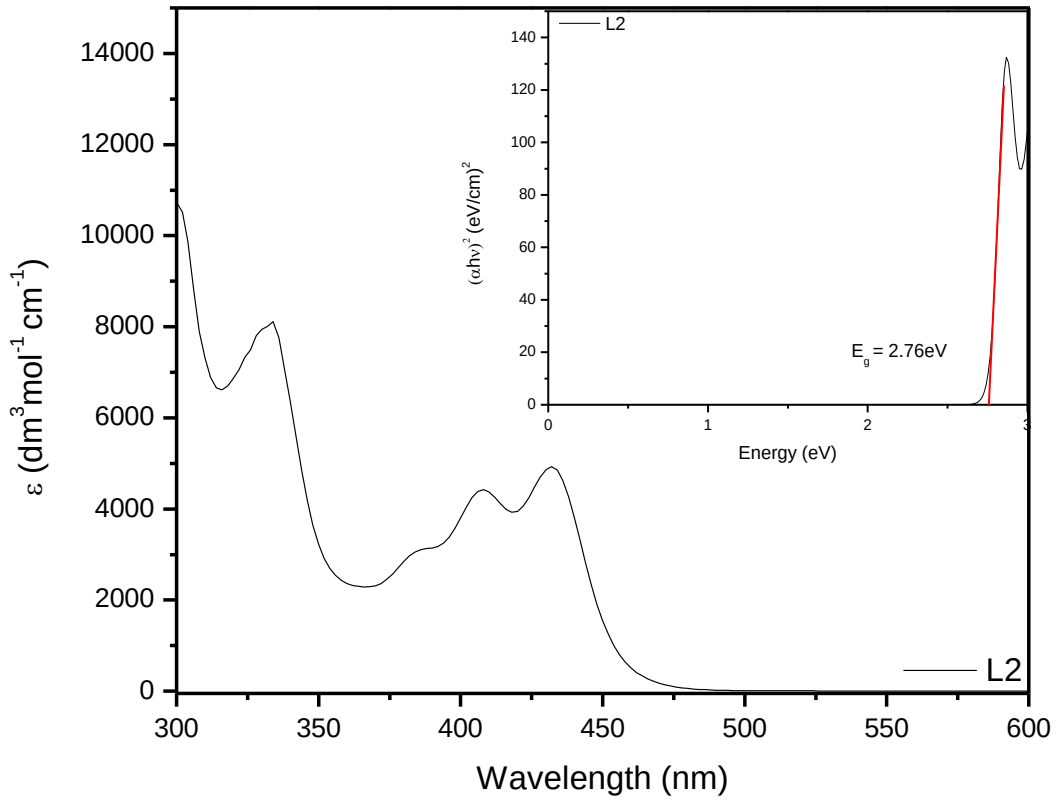

Figure S7: UV-Vis spectra and Tauc plot of **L2** [21, 29, 32].

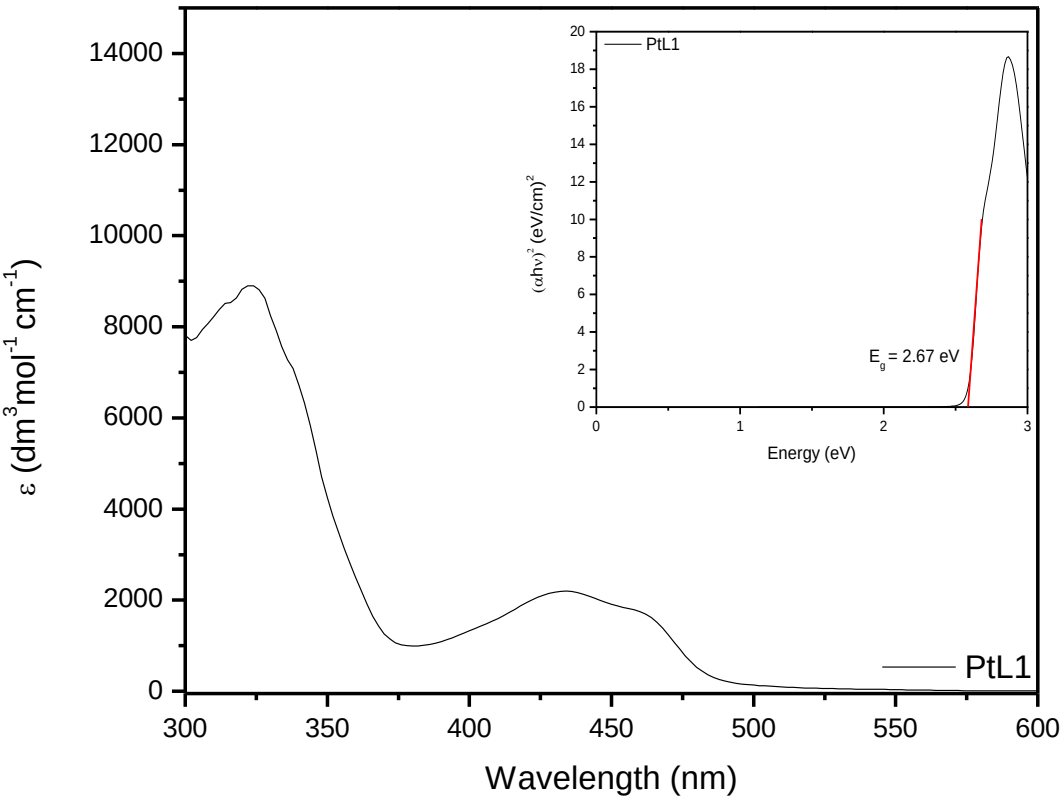

Figure S8: UV-Vis spectra and Tauc plot of **PtL1** [21, 29, 32].

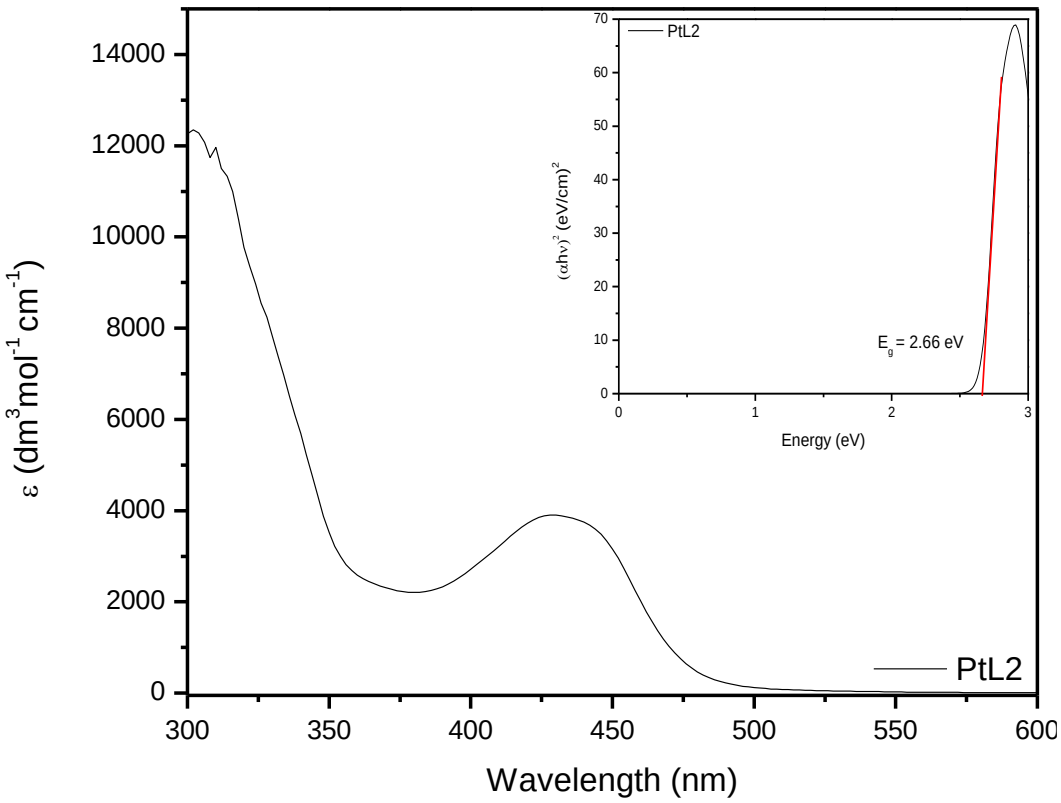

Figure S9: UV-Vis spectra and Tauc plot of **PtL2** [21, 29, 32].

Structural characterization

	PtL1	**PtL2**
Empirical formula	$C_{27}H_{24}N_2O_2Pt$	$C_{27}H_{24}N_2O_3Pt$
Formula weight	603.57	619.57
Crystal Color	yellow	orange
Crystal size (mm^3)	0.04 × 0.08 × 0.14	0.118 × 0.08 × 0.069
Crystal system	monoclinic	orthorhombic
Space group	$P2_1/c$	$P2_12_12_1$
Temperature (K)	293(2)	293(2)
a (Å)	13.74289(8)	7.84920(10)
b (Å)	12.23957(9)	12.9055(2)
c (Å)	13.11559(9)	21.3423(3)
α (°)	90	90
β (°)	98.9538(6)	90
γ (°)	90	90
Volume ($Å^3$)	2179.25(3)	2161.93(5)
Z	4	4
ϱ_{calc} (g/cm^3)	1.840	1.904
μ (mm^{-1})	12.261	12.415
Reflections collected	49243	34483
F(000)	1176.0	1208.0
Radiation	Cu Kα (λ = 1.54184 Å)	Cu Kα (λ = 1.54184 Å)
2Θ range for data collection/°	6.51 to 136.81	8.006 to 137.16
Index ranges	-16 ≤ h ≤ 16, -14 ≤ k ≤ 14, -15 ≤ l ≤ 15	-9 ≤ h ≤ 9, -15 ≤ k ≤ 15, -25 ≤ l ≤ 25
Independent reflections	4008 [R_{int} = 0.0460, R_{sigma} = 0.0178]	3986 [R_{int} = 0.0474, R_{sigma} = 0.0225]
Data/restraints /parameters	4008/0/310	3986/0/301

Goodness-of-fit on F^2	0.985	1.072
Final R indexes [I>=2σ (I)]	R_1 = 0.0228, wR_2 = 0.0651	R_1 = 0.0213, wR_2 = 0.0476
Final R indexes [all data]	R_1 = 0.0250, wR_2 = 0.0669	R_1 = 0.0219, wR_2 = 0.0479
Largest diff. peak/hole / e $Å^{-3}$	0.58/-0.91	0.95/-0.95

Table S2: Crystallographic data of **PtL1**, and **PtL2**.

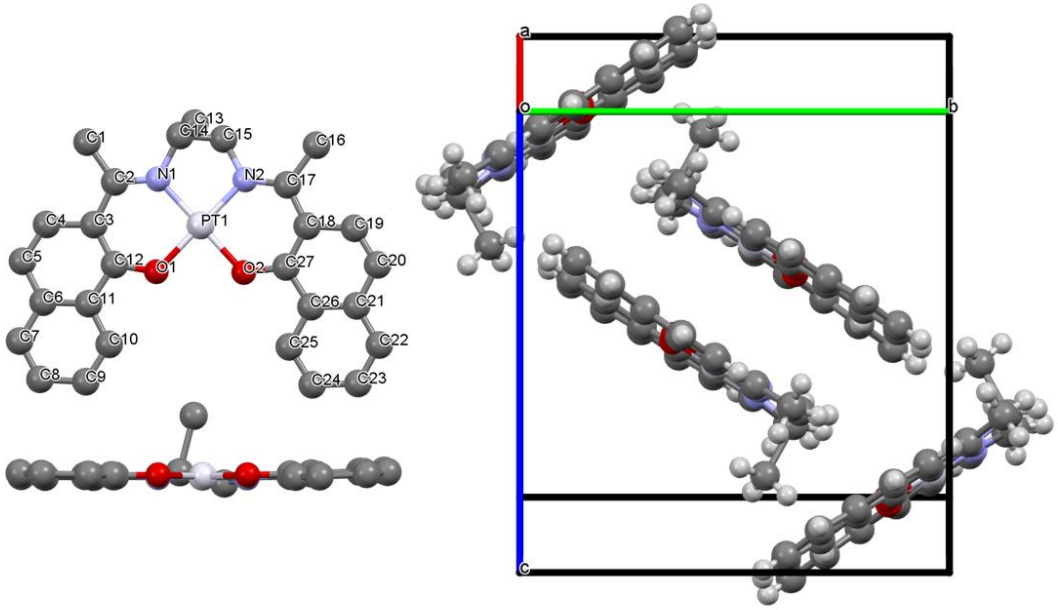

Figure S10: Front, side, and packing of **PtL1** crystal structure.

	L1	**PtL1**
M-O1		1.977(3)
M-O2		1.978(2)
M-N1		1.963(4)
M-N2		1.962(4)
O1-C12	1.2917(16)	1.303(5)
O2-C27	1.2923(17)	1.301(4)
N1-C2	1.3141(18)	1.293(6)
N1-C14	1.4722(18)	1.58(2)
N2-C15	1.4624(18)	1.47(1)
N2-C17	1.3121(18)	1.305(6)
C27-C18-C17-N2		1.65
C12-C3-C2-N1		0.69
O1-M-N1		93.1(1)
O1-M-O2		85.5(1)
O1-M-N2		179.5(2)
O2-M-N2		94.0(1)
N1-M-O2		178.8(1)
N2-M-N1		86.6(2)
O1-N1-N2-O2		-0.64
O1-N1-N2-M		-179.83
M•••M		8.284
τ_4	-	0.008
τ'_4	-	0.009

Table S3: Selected bond lengths and bond angles of **L1**, and **PtL1**.[26]

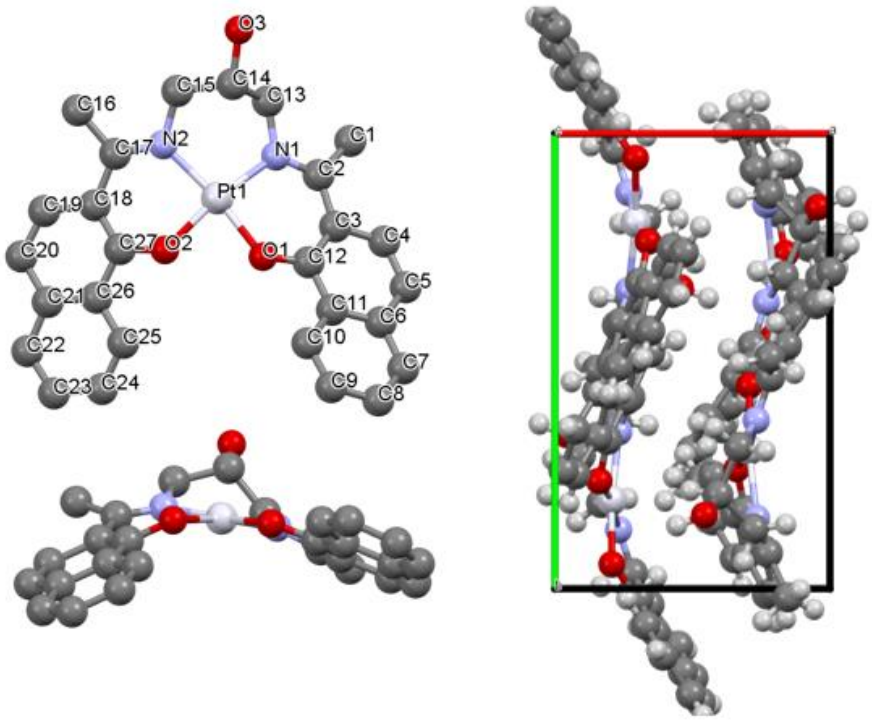

Figure S11: Front, side, and packing of **PtL2** crystal structure.

	PtL2
M-O1	1.995(4)
M-O2	1.976(5)
M-N1	2.019(5)
M-N2	2.007(5)
O1-C12	1.300(8)
O2-C27	1.296(7)
O3-C14	1.424(8)
N1-C2	1.295(9)
N1-C13	1.483(8)
N2-C15	1.461(8)
N2-C17	1.302(8)
C27-C18-C17-N2	20.40
C12-C3-C2-N1	0.65
O1-M-N1	89.8(8)
O1- M-O2	81.82(17)
O1- M-N2	170.4(2)
O2- M-N2	91.2(2)
N1- M-O2	170.4(2)
N2- M-N1	97.6(2)
O1-N1-N2-O2	7.52
O1-N1-N2-M	173.92
M•••M	4.177
τ_4	0.13
τ'_4	0.13

Table S4: Selected bond lengths and bond angles of **PtL2**.

DFT calculations

	L1 keto (DFT)	**L1 enol (DFT)**	**PtL1 (DFT)**
Pd1-O1			2.000
Pd1-O2			2.007
Pd1-N1			1.993
Pd1-N2			1.978
O1-C12	1.276	1.333	1.297
O2-C27	1.246	1.372	1.299
N1-C2	1.332	1.296	1.322
N1-C14	1.461	1.459	1.490
N2-C15	1.456	1.453	1.467
N2-C17	1.365	1.283	1.317
C27-C18-C17-O2	2.2	143.1	3.1
C12-C3-C2-O1	0.9	0.0	4.4
O1-Pd1-N1			94.0
O1- Pd1-O2			87.1
O1- Pd1-N2			179.1
O2- Pd1-N2			92.6
N1- Pd1-O2			176.3
N2- Pd1-N1			86.4
O1-N1-N2-O2			2.9
O1-N1-N2-M			179.2
O1•••O2	5.256	6.933	2.760

Table S5: Selected bond lengths and bond angles of **L1, PdL1**, and **PtL1** optimized geometry.

	L2 enol (DFT)	**L2 keto (DFT)**	**PtL2 (DFT)**
Pd1-O1			2.010
Pd1-O2			2.011
Pd1-N1			2.028
Pd1-N2			2.027
O1-C12	1.371	1.247	1.298
O2-C27	1.333	1.280	1.297
O3-C14	1.433	1.428	1.433
N1-C2	1.282	1.361	1.322
N1-C13	1.455	1.455	1.469
N2-C15	1.453	1.450	1.469
N2-C17	1.298	1.334	1.323
C19-C18-C17-O2	1.0	0.7	10.9
C4-C3-C2-O1	1.5	1.8	10.7
O1-Pd1-N1			88.6
O1- Pd1-O2			86.2
O1- Pd1-N2			174.7
O2- Pd1-N2			88.6
N1- Pd1-O2			174.8
N2- Pd1-N1			96.6
O1-N1-N2-O2			0.1
O1-N1-N2-M			178.9
O1•••O2	3.710	6.724	2.748

Table S6: Selected bond lengths and bond angles of **L2, PdL2,** and **PtL2** optimized geometry.

Species	**HOMO (eV)**	**LUMO (eV)**	**E_g (eV)**
L1 (keto)	-5.15	-2.07	3.09
L1 (enol)	-5.38	-1.52	3.86
L2 (keto)	-5.03	-2.19	2.84
L2 (enol)	-5.60	-1.65	3.95
PdL1	-5.05	-1.67	3.37
PtL1	-4.94	-1.78	3.17
PdL2	-5.17	-1.74	3.43
PtL2	-5.09	-1.72	3.37

Table S7: Theoretical HOMO, LUMO, and bandgap (E_g) values of the studied compounds at B3LYP/6-31+G* level of theory.

Electrochemical studies

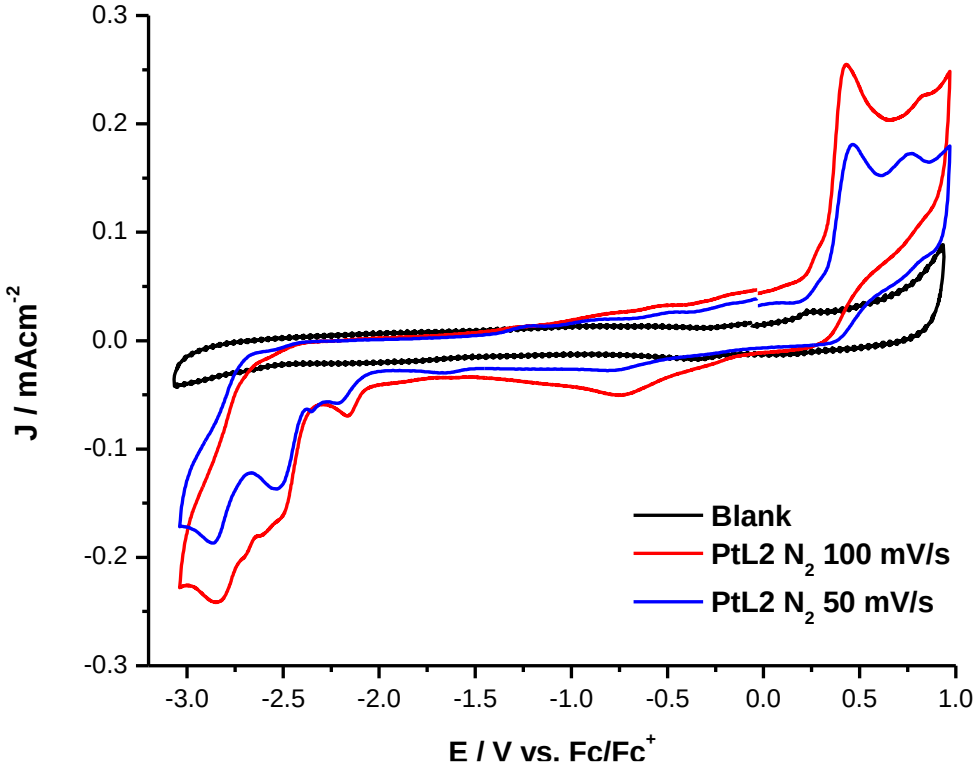

Figure S12: Cyclic voltammograms of 1 mM **PtL2** at 100 mV/s and 50 mV/s in DMF with 0.1M TBAPF6 under N_2 inert atmosphere.

	$E_{ox,1}$ (V vs Fc/Fc⁺)	$E_{ox,2}$ (V vs Fc/Fc⁺)	$E_{ox,3}$ (V vs Fc/Fc⁺)	$E_{red,1}$ (V vs Fc/Fc⁺)	$E_{red,2}$ (V vs Fc/Fc⁺)	$E_{red,3}$ (V vs Fc/Fc⁺)	$E_{red,4}$ (V vs Fc/Fc⁺)
L1	0.47	-0.85	-	-2.49	-	-	-
L2	0.35	-	-	-2.38	-	-	-
PtL1	0.38	-2.40	-1.69	-2.55	-2.90	-	-
PtL2*	0.43	-	-	-2.21	-2.53	-2.86	-

*Redox peaks were determined at a scan rate of 50 mV/s.

Table S8: Redox processes of **L1**, **L2**, **PtL1,** and **PtL2** referenced to ferrocene internal standard under N_2 saturation.

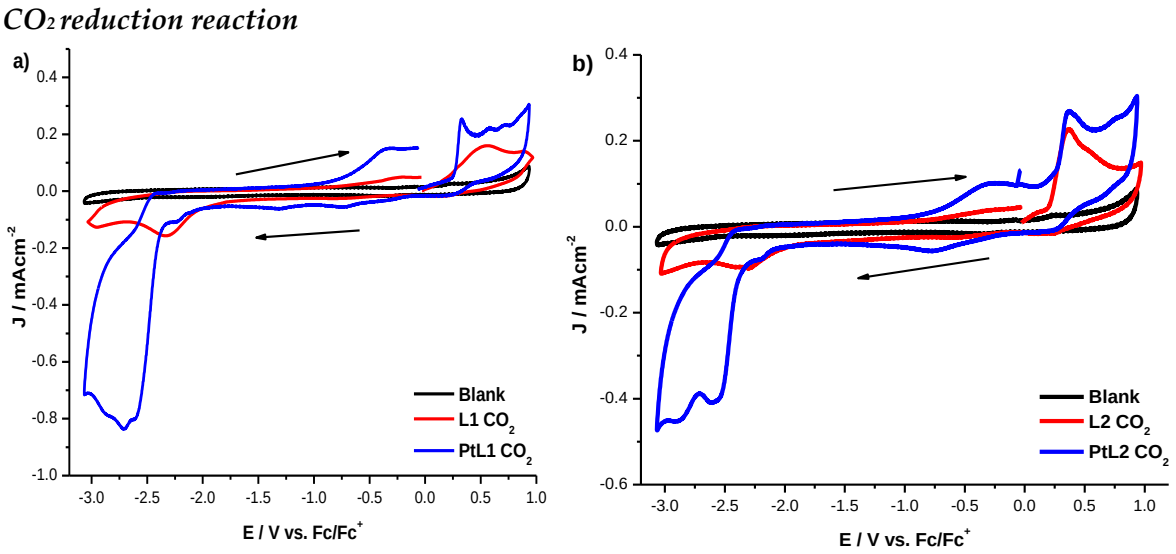

Figure S13: Cyclic voltammograms of 1 mM of **L1**, **L2**, **PtL1**, and **PtL2** at 100 mV/s in DMF with 0.1M TBAPF6. a) **L1** and b) **L2** samples under CO_2 atmosphere.

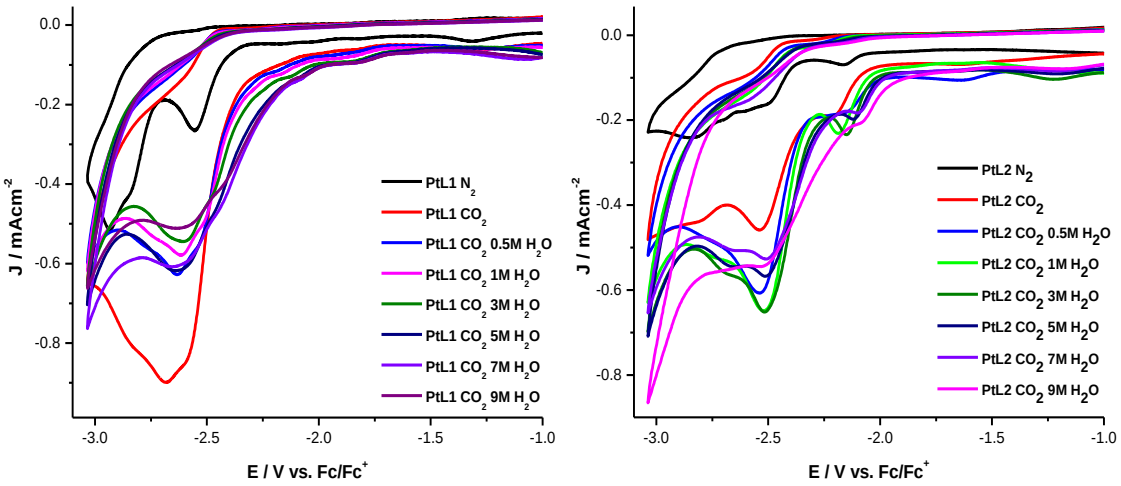

Figure S14: Cyclic voltammograms of 1 mM of a) **PtL1** and b) **PtL2** at 100 mV/s in DMF with 0.1M TBAPF6 under CO_2 saturation and addition of water as a sacrificial proton source.

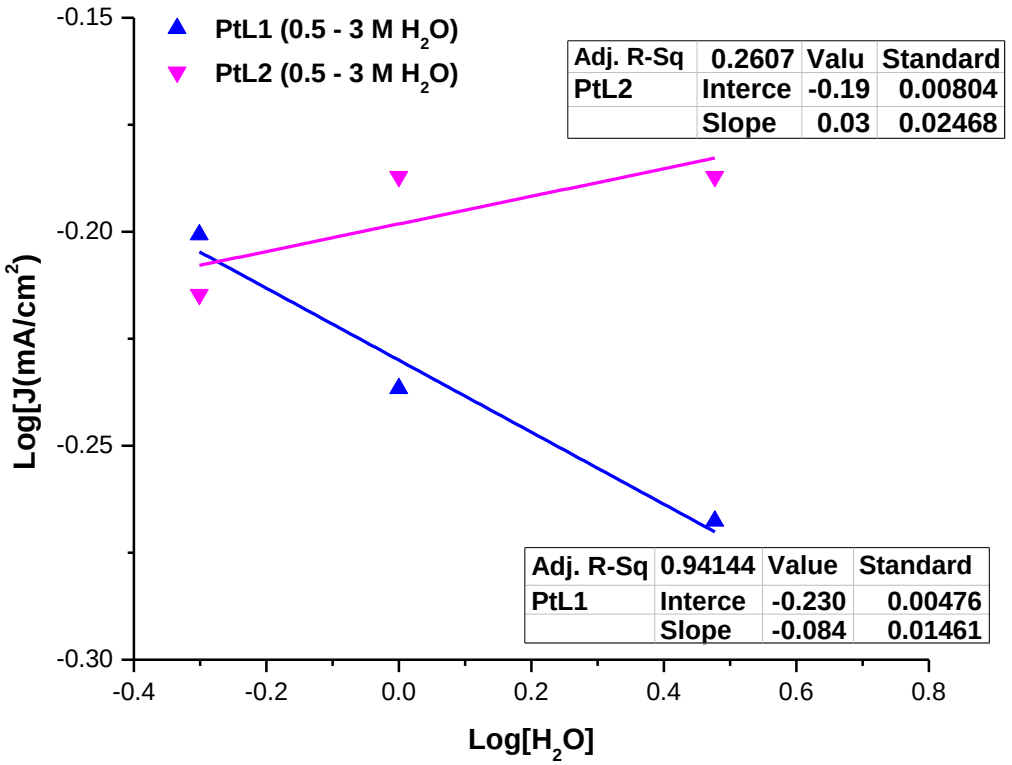

Figure S15: Log-Log plot of CV under CO_2 saturation and various H_2O of **PtL1**, and **PtL2** at 1mM [39, 40].

$$[H_2O][CO_2][Cat] \longrightarrow \text{products}$$

$$r = k[H_2O][CO_2][Cat]$$

$$k' = k[CO_2][Cat]$$

$$r = k'[H_2O]$$

$$\ln[H_2O] = \ln[H_2O]_0 - kt$$

first order kinetics

Bulk Electrolysis

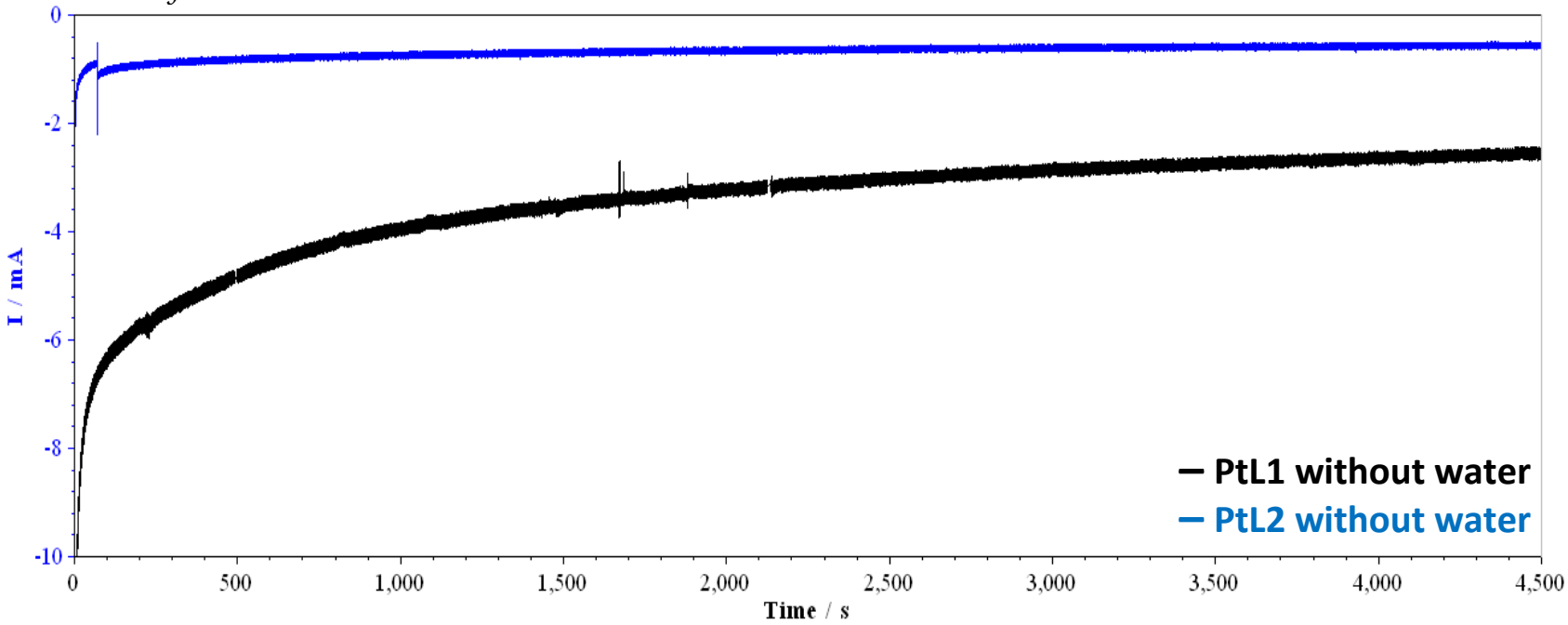

Figure S16: Bulk electrolysis of 1 mM of **PtL1** (black) at -2.7 V vs Fc/Fc^+ and **PtL2** (blue) -2.5 V vs Fc/Fc^+ for 4500 s in DMF with 0.1 M $TBAPF_6$ under CO_2 saturation.

PtL1	**Injection**	**Time (s)**	**[CO] (mol)**	**Charge (C)**	**FE%**
no H2O	1	1800	1.93E-06	7.97397	4.68
-2.7	2	4080	4.16E-06	14.6013	5.49
PtL2	**Injection**	**Time (s)**	**[CO] (mol)**	**Charge (C)**	**FE%**
no H2O	1	1800	5.81E-06	1.42391	3.93
-2.5	2	3600	2.90E-07	2.49933	4.43

Table S9: Product quantification for CO_2RR under aprotic conditions of 1 mM of **PtL1** and **PtL2**.

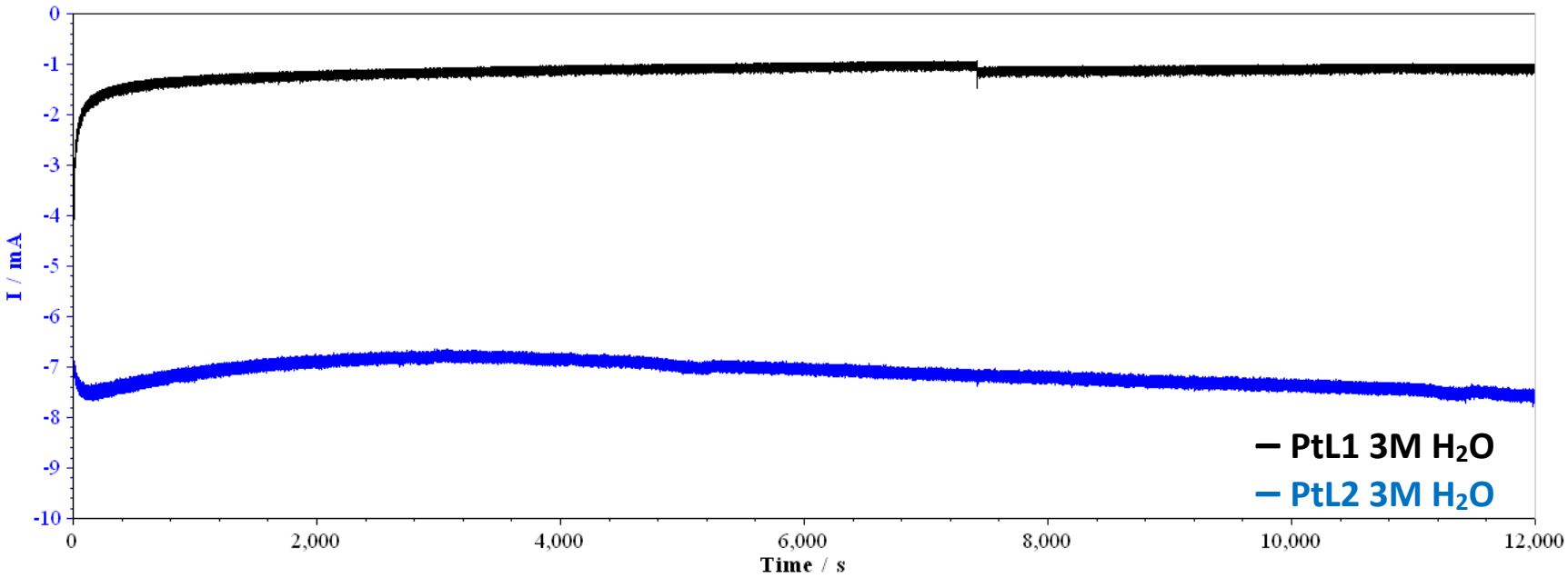

Figure S17: Bulk electrolysis of 1 mM of **PtL1** (black) at -2.7 V vs Fc/Fc^+ and **PtL2** (blue) -2.5 V vs Fc/Fc^+ for 12000 s in DMF with 0.1M $TBAPF_6$ under CO_2 saturation.

	Injection	Time (s)	[CO] (mol)	Charge (C)	FE %
PtL1 -2.7 3M H_2O	1	1800	2.44E-07	2.56739	1.84
	2	3600	5.63E-07	4.6751	2.32
	3	7200	1.93E-06	8.49651	4.39
	4	9000	2.86E-06	10.4846	5.27
	5	10800	3.26E-06	12.4416	5.05
	Injection	**Time (s)**	**[CO] (mol)**	**Charge (C)**	**FE %**
PtL2 -2.5 3M H_2O	1	1800	2.82E-05	12.9496	41.99
	2	3600	4.48E-05	25.2499	34.26
	3	7200	6.62E-05	50.4139	25.32
	4	9000	6.75E-05	63.4254	20.53
	5	10800	6.81E-05	76.694	17.13

Table S10: Product quantification for CO_2RR under protic conditions (3M H_2O) of 1 mM of **PtL1** and **PtL2.**

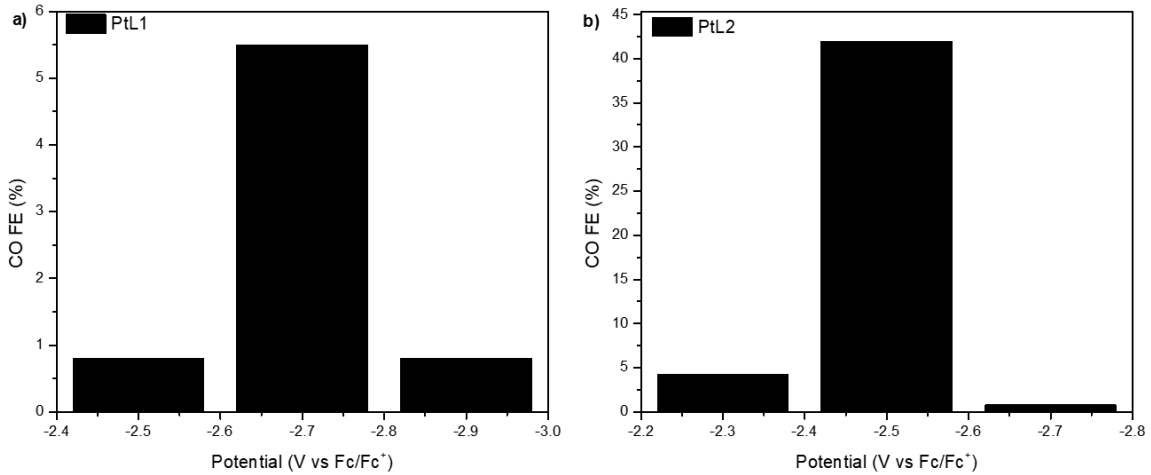

Figure S18: CO formation at different potentials for a) **PtL1** (-2.3, -2.5, and -2.7 V vs Fc/Fc^+) and b) **PtL2** (-2.5, -2.7, and -2.9 V vs Fc/Fc^+). Conditions: working electrode and counter electrode were graphite rods, reference electrode was 0.01 M $AgNO_3$, and 3 M H_2O.

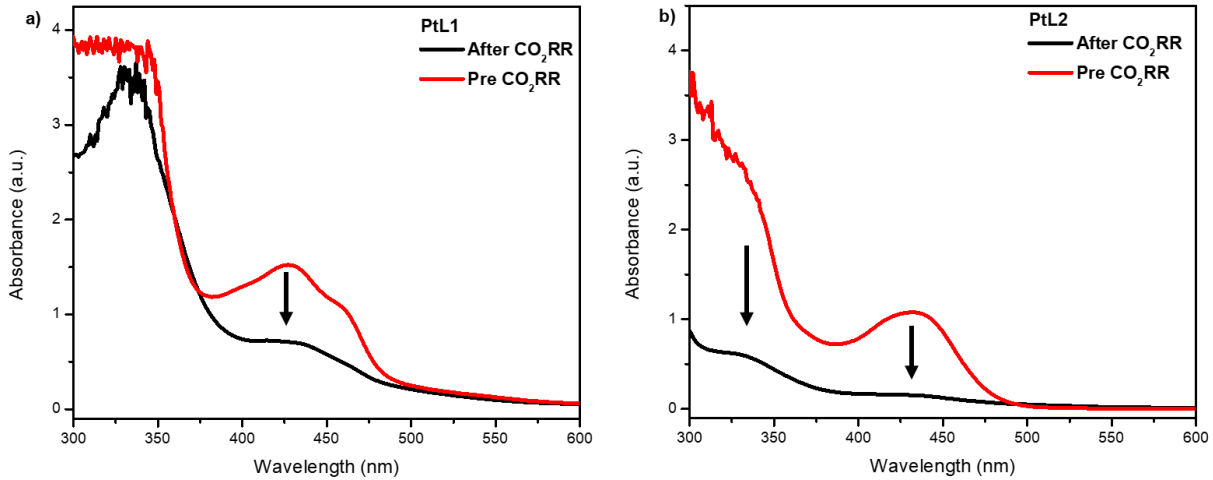

Figure S19: UV-Vis spectra before and after CO_2RR a) **PtL1** and b) **PtL2. NOTE:** Solutions after electrolysis were diluted from 1 mM to 0.3 mM to avoid UV-Vis signal saturation using the 0.1 M $TBAPF_6$ in DMF electrolyte solution.